RAPID COMMUNICATION

Large linear magnetoresistance in a new Dirac material $BaMnBi_2$*

Yi-Yan Wang(王义炎)[1,2,†], Qiao-He Yu(郁巧鹤)[1,2,†], and Tian-Long Xia(夏天龙)[1,2,‡]

[1] Department of Physics, Renmin University of China, Beijing 100872, China

[2] Beijing Key Laboratory of Opto-electronic Functional Materials & Micro-nano Devices, Renmin University of China, Beijing 100872, China

(Received 23 June 2016; revised manuscript received 4 August 2016; published online 25 August 2016)

Dirac semimetal is a class of materials that host Dirac fermions as emergent quasi-particles. Dirac cone-type band structure can bring interesting properties such as quantum linear magnetoresistance and large mobility in the materials. In this paper, we report the synthesis of high quality single crystals of $BaMnBi_2$ and investigate the transport properties of the samples. $BaMnBi_2$ is a metal with an antiferromagnetic transition at $T_N = 288$ K. The temperature dependence of magnetization displays different behavior from $CaMnBi_2$ and $SrMnBi_2$, which suggests the possible different magnetic structure of $BaMnBi_2$. The Hall data reveals electron-type carriers and a mobility $\mu(5\ \mathrm{K}) = 1500\ \mathrm{cm}^2/\mathrm{V}\cdot\mathrm{s}$. Angle-dependent magnetoresistance reveals the quasi-two-dimensional (2D) Fermi surface in $BaMnBi_2$. A crossover from semiclassical MR $\sim H^2$ dependence in low field to MR $\sim H$ dependence in high field, which is attributed to the quantum limit of Dirac fermions, has been observed in magnetoresistance. Our results indicate the existence of Dirac fermions in $BaMnBi_2$.

Keywords: topological material, Dirac semimetal, magnetoresistance

PACS: 75.47.–m, 73.43.Qt, 75.30.Gw **DOI:** 10.1088/1674-1056/25/10/107503

1. Introduction

Dirac material is a group of compounds whose low-energy excitation behaves as massless Dirac particles.[1] In recent years, a variety of Dirac materials have been discovered, such as graphene,[2] three-dimensional (3D) topological insulators $Bi_{1-x}Sb_x$, Bi_2Se_3, and Bi_2Te_3,[3,4] and Dirac semimetals Na_3Bi,[5] Cd_3As_2.[6–9] The energy spectrum of Dirac materials exhibits linear behavior and can be described by relativistic Dirac equation. More interestingly, when the time reversal symmetry or space inversion symmetry is broken, Dirac semimetals (DSM) evolve into Weyl semimetals (WSM), whose extraordinary properties such as Fermi arc and chiral anomaly have attracted great attention.[10–24] One interesting consequence of the linear energy dispersion is quantum transport phenomena. For Dirac materials, a moderate magnetic field can compel all carriers occupy the lowest Landau level and lead to the quantum linear magnetoresistance (*MR*).[25,26]

In Dirac materials, there is a class of ternary 112 type compounds such as $CaMnBi_2$,[27–30] $SrMnBi_2$,[31–34] $EuMnBi_2$,[35,36] and $LaAgBi_2$,[37] which have been researched deeply. More recently, time-reversal symmetry breaking Weyl state has been suggested to exist in $YbMnBi_2$,[38] and $Sr_{1-y}Mn_{1-z}Sb_2$[39] is also identified as a promising candidate of WSM. Among these materials, the Bi/Sb square net is a common feature and has been considered as the platform that hosts Dirac/Weyl fermions. Therefore, it is of considerable interest to explore new materials which have similar structure and further study their physical properties.

In this work, we have synthesized the single crystals of $BaMnBi_2$ and investigated the transport properties. Hall resistivity shows carriers in $BaMnBi_2$ are electron type. Magnetic property measurement indicates the magnetic structure of $BaMnBi_2$ may be slightly different from that of $SrMnBi_2$ or $CaMnBi_2$. Angle-dependent *MR* implies the anisotropic quasi-two-dimensional Fermi surface in $BaMnBi_2$. The in-plane *MR* displays a crossover from semiclassical quadratic field dependence to linear field dependence with the increase of magnetic field. The linear *MR* indicates the possible existence of Dirac fermions in this material. It is worth doing ARPES experiments to check whether $BaMnBi_2$ is a Weyl semimetal.

2. Experiment and crystal structure

Single crystals of $BaMnBi_2$ were grown from Bi flux. The mixtures of Ba, Mn and Bi were placed in a crucible and sealed in a quartz tube with a ratio of Ba:Mn:Bi=1:1:6. The quartz tube was heated to 1180 °C in 60 h, held there for 30 h, and cooled to 370 °C at a rate of 3 °C/h, and then the excess Bi-flux was removed by centrifuging. Elemental analysis was performed using energy dispersive x-ray spectroscopy (EDS, Oxford X-Max 50). The determined atomic proportion was consistent with the composition of $BaMnBi_2$ within instrumental

*Project supported by the National Natural Science Foundation of China (Grant No. 11574391), the Fundamental Research Funds for the Central Universities, and the Research Funds of Renmin University of China (Grant No. 14XNLQ07).

†These authors contribute equally to this work.

‡Corresponding author. E-mail: tlxia@ruc.edu.cn

© 2016 Chinese Physical Society and IOP Publishing Ltd

error. Single crystal x-ray diffraction (XRD) pattern was collected from a Bruker D8 Advance x-ray diffractometer using Cu K_α radiation. Resistivity measurements were performed on a Quantum Design physical property measurement system (QD PPMS-14T) and the magnetic properties were measured with vibrating sample magnetometer (VSM) option.

$BaMnBi_2$ is isostructural with $SrMnBi_2$. As shown in Fig. 1(a), the crystal structure of $BaMnBi_2$ is comprised of alternating MnBi and BaBi layers.[40] In the MnBi layer, each Mn atom is surrounded by four Bi atoms, which form the $MnBi_4$ tetrahedra. In the BaBi layer, Bi atoms are separated and form a square net (highlighted by red atoms). Figure 1(c) shows the x-ray diffraction pattern of a $BaMnBi_2$ single crystal on the (00l) plane. An additional small peak at about 27.2° also has been observed. It may come from the residual Bi flux on the surface. The inset is an optical image of a representative crystal.

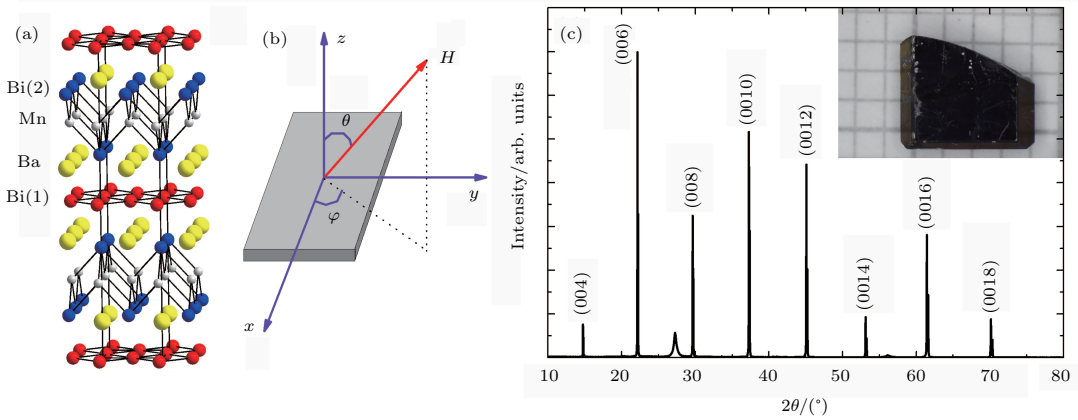


Fig. 1. (color online) (a) The crystal structure of $BaMnBi_2$. (b) The definition of polar angle θ and azimuthal angle φ. (c) Single crystal x-ray diffraction pattern of a $BaMnBi_2$ crystal, showing only the (00l) reflections. The inset is an image of a typical single crystal with a scale of 4 mm.

3. Results and discussion

Both the in-plane resistivity $\rho_{xx}(T)$ and out-plane resistivity $\rho_z(T)$ exhibit a simple metallic behavior as shown in Fig. 2(a). The out-plane resistivity is nearly 50 times the in-plane resistivity in a range of 2.5 K–300 K. Such a significant anisotropy suggests quasi-2D electronic band structure in $BaMnBi_2$.

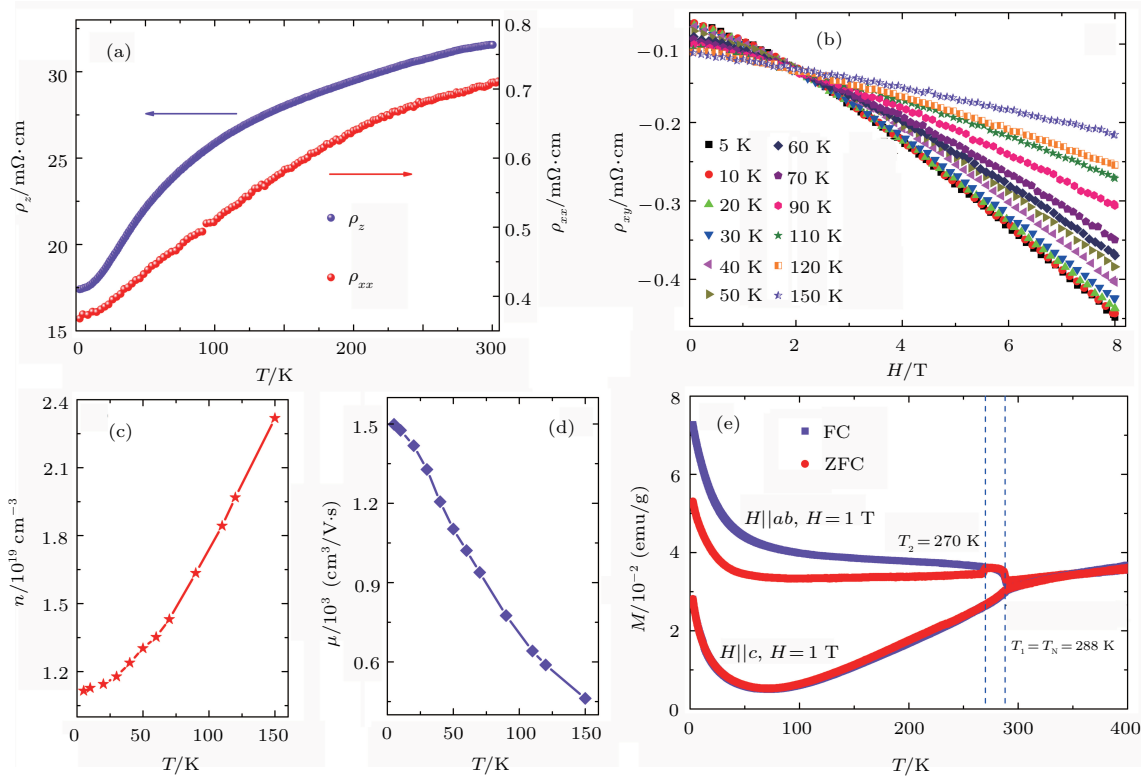


Fig. 2. (color online) (a) Temperature dependence of in-plane resistivity $\rho_{xx}(T)$ and out-plane resistivity $\rho_z(T)$. (b) Hall resistivity ρ_{xy} versus magnetic field H with the temperature T from 5 K to 150 K. (c) and (d) Temperature dependence of carrier concentration and mobility, respectively. (e) Magnetization versus temperature with the magnetic field $H = 1$ T applied parallel to ab plane (up) and c axis (down) under zero field cooling (ZFC) (red) and field cooling (FC) (violet) conditions. The dashed lines denote two anomalous temperatures.

Figure 2(b) plots the magnetic field dependence of Hall resistivity $\rho_{xy}(H)$ measured at various temperatures. The negative slope of ρ_{xy} suggests that the dominant charge carriers in $BaMnBi_2$ are electrons. Single band model has been employed to analyze the Hall effect data. The carrier concentration and carrier mobility are shown in Figs. 2(c) and 2(d) respectively. The carrier concentration is given by $n = 1/eR_H$, and the Hall coefficient R_H is obtained by $R_H = \rho_{xy}(8\ \mathrm{T})/H$. At 5 K, the carrier concentration is $1.1 \times 10^{19}\ \mathrm{cm}^{-3}$. We calculate the carrier mobility by $\mu = 1/en\rho_{xx}(0\ \mathrm{T})$. With temperature reduced, the mobility becomes larger and reaches $1500\ \mathrm{cm}^2/\mathrm{V}\cdot\mathrm{s}$ at 5 K.

Figure 2(e) presents the temperature dependence of magnetization of $BaMnBi_2$ measured under zero field cooling (ZFC) and field cooling (FC) conditions with an applied field $H = 1$ T parallel to *ab* plane and *c* axis respectively. Similar to $CaMnBi_2$ and $SrMnBi_2$,[33,34] there are two anomalous temperatures in $BaMnBi_2$. $T_1 = T_N = 288$ K is the temperature of antiferromagnetic transition, below T_1 the magnetization exhibits strong anisotropy, the linear temperature dependence of magnetization with positive slope above T_1 indicates strong antiferromagnetic correlations.[41] There is a ZFC–FC splitting for magnetic field parallel to *ab* plane when $T < T_2 = 270$ K. This is quite different from the behavior in $CaMnBi_2$ or $SrMnBi_2$, in which the ZFC–FC splitting occurs when the field is parallel to *c* axis. The difference implies that the magnetic structure of $BaMnBi_2$ may be slightly different from that of $CaMnBi_2$ or $SrMnBi_2$.

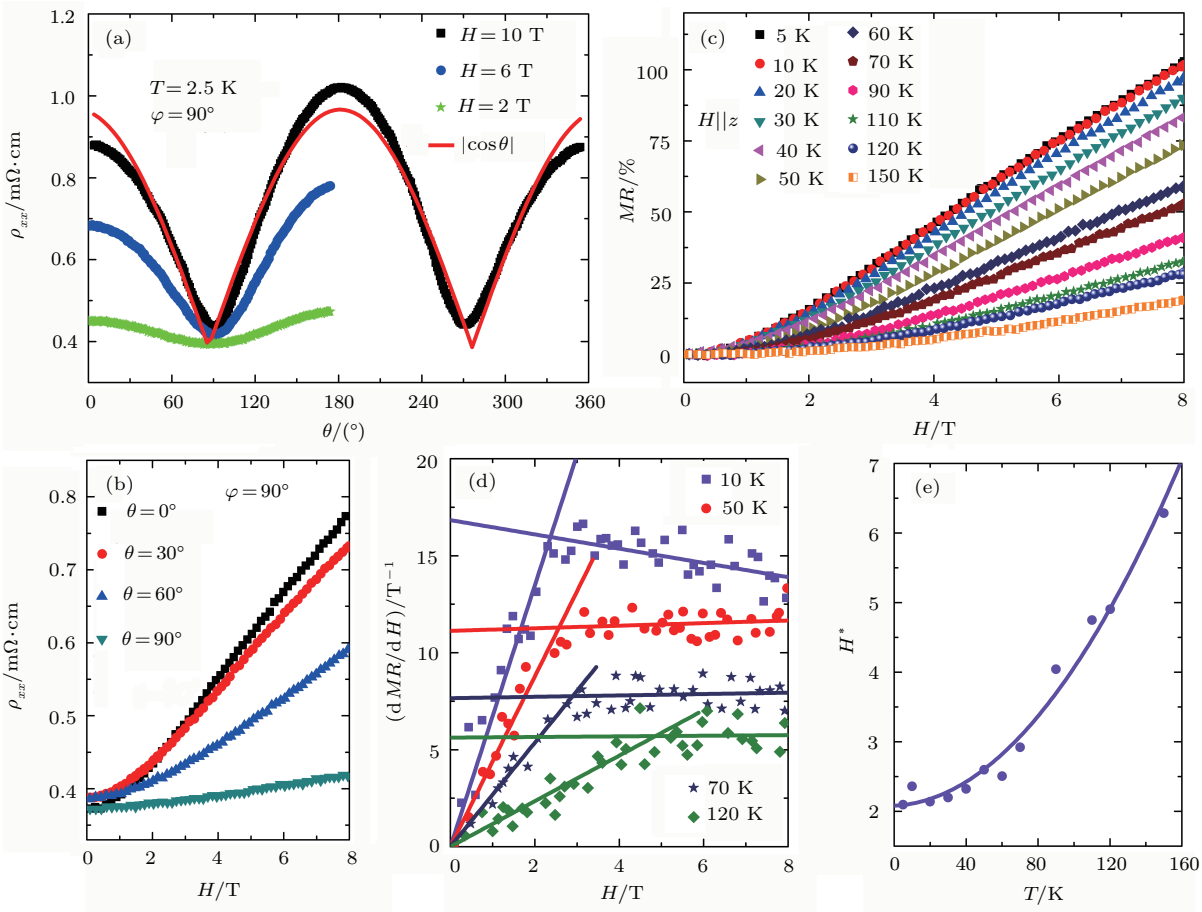


Fig. 3. (color online) (a) Polar angle θ dependence of in-plane resistivity ρ_{xx} at $H = 10$, 6, 2 T. The temperature and azimuthal angle are fixed at $T = 2.5$ K and $\varphi = 90°$ respectively. The red curve is the fitting of cosine function. (b) Magnetic field H dependence of in-plane resistivity ρ_{xx} with different polar angle θ at 2.5 K. (c) In-plane magnetoresistance MR versus magnetic field H with the temperature from 5 K to 150 K. (d) The field derivative of the MR as a function of magnetic field H. The straight lines in low field regions are linear fitting results using the relationship $MR = A_2H^2$. Lines in high field regions are fitting results using $MR = A_1H + O(H^2)$. The intersection of fitting lines in low field and high field is defined as critical point H^*. (e) Temperature dependence of critical point H^*. The solid curve is the fit to the equation $H^* = (E_F + k_BT)^2/2ev_F^2\hbar$.

The carriers of a metal in magnetic field are subject to the Lorentz force. The Lorentz force affects the carriers' momentum components in the plane perpendicular to the field and MR is partially determined by the mobility in this plane. The carriers in a quasi-2D material will only be affected by the magnetic field component $H|\cos\theta|$. Figure 3(a) shows the angular-dependent in-plane MR measured in different magnetic fields. When $\theta = 0°, 180°$ (field parallel to *c* axis), MR has the maximum value. With the increase of the polar angle θ, MR decreases gradually and reaches the minimum value when $\theta = 90°$. The $|\cos\theta|$ function behavior of the whole curve indicates the existence of a quasi-2D Fermi surface in $BaMnBi_2$. The small deviation implies the existence of 3D electronic transport in $BaMnBi_2$.

Figure 3(c) shows the in-plane MR as a function of magnetic field at different temperatures. The MR exhibits quantum linear behavior in high field and semiclassical quadratic dependence in low field.[42] The transition from semiclassical to quantum can be seen more clearly from the field derivative of the MR [Fig. 3(d)]. Initially, dMR/dH is proportional to H, which indicates a semiclassical H^2-dependent MR. With the increase of magnetic field, the field crosses a critical point H^* and dMR/dH nearly becomes a constant. This implies that MR follows linear field dependence plus a small quadratic term in high field, namely $MR = A_1H + O(H^2)$. The linear MR suggests the existence of Dirac fermions in $BaMnBi_2$.[43–46]

A sufficiently strong perpendicular magnetic field can cause the complete quantization of orbit of Dirac fermions and the quantized Landau level can be described as $E_n = \mathrm{sgn}(n)v_F\sqrt{2e\hbar H|n|}$, where v_F is the Fermi velocity and n is the Landau index. So the energy splitting between the first and lowest Landau level is $\Delta = \pm v_F\sqrt{2e\hbar H}$. At a specific temperature T, with the increase of field H, the energy splitting becomes larger than the Fermi energy E_F and the thermal fluctuations k_BT. As a result, all carriers will occupy the lowest Landau level and reach the quantum limit. With these two relationships combined, we can get the temperature dependence of the critical magnetic field $H^* = (E_F + k_BT)^2/2e\hbar v_F^2$.[47] However, the condition for absolute quantum limit is $n < (eH/\hbar)^{3/2}$, where n is the carrier concentration. Substituting the electron concentration $n(5\ \mathrm{K}) = 1.1 \times 10^{19}\ \mathrm{cm}^{-3}$ obtained from the Hall measurement into the expression, we get the value $H > 32.5$ T. Although the system does not enter the absolute quantum limit in our situation, the linear quantum MR also could appear at lower field with more than one Landau level filled, which also has been observed in previous research on InSb.[45] In addition, considering the relationship between T and H^* can be well fitted by the equation as shown in Fig. 3(e), it is suggested that the linear MR in $BaMnBi_2$ originates from Dirac fermions.

4. Summary

In summary, single crystals of $BaMnBi_2$ have been grown. Resistivity, Hall resistivity, magnetic property and magnetoresistance have been measured and analyzed. Compared with $CaMnBi_2$ and $SrMnBi_2$, the different behavior of magnetization brings the possibly different magnetic structure of $BaMnBi_2$. Quasi-2D electronic transport is also observed in angle-dependent MR. The crossover from semiclassical parabolic field-dependent MR in low field to linear field-dependent MR in high field can be explained by combining semiclassical and quantum magnetoresistance. Our results clearly indicate the existence of Dirac fermions in $BaMnBi_2$.

Note added When the paper was being finalized, we noticed one similar related work on $BaMnBi_2$,[48] where the Shubnikov–de Hass oscillation is also observed under high magnetic field. However, the angle-dependent resistivity in their work is different from ours and deviates greatly from the $|\cos\theta|$ relationship, which may be caused by misaligned leads on the samples besides the contribution from 3D Fermi surface.

Acknowledgment

We thank Professor J F Wang for his help in our attempt to obtain high field data.

References

[1] Wehling T O, Black-Schaffer A M and Balatsky A V 2014 *Adv. Phys.* **63** 1
[2] Castro Neto A H, Guinea F, Peres N M R, Novoselov K S and Geim A K 2009 *Rev. Mod. Phys.* **81** 109
[3] Hasan M Z and Kane C L 2010 *Rev. Mod. Phys.* **82** 3045
[4] Qi X L and Zhang S C 2011 *Rev. Mod. Phys.* **83** 1057
[5] Liu Z K, Zhou B, Zhang Y, Wang Z J, Weng H M, Prabhakaran D, Mo S K, Shen Z X, Fang Z, Dai X, Hussain Z and Chen Y L 2014 *Science* **343** 864
[6] Borisenko S, Gibson Q, Evtushinsky D, Zabolotnyy V, Büchner B and Cava R J 2014 *Phys. Rev. Lett.* **113** 027603
[7] Neupane M, Xu S Y, Sankar R, Alidoust N, Bian G, Liu C, Belopolski I, Chang T R, Jeng H T, Lin H, Bansil A, Chou F and Hasan M Z 2014 *Nat. Commun.* **5** 3786
[8] Liang T, Gibson Q, Ali M N, Liu M, Cava R J and Ong N P 2015 *Nat. Mater.* **14** 280
[9] He L P, Hong X C, Dong J K, Pan J, Zhang Z, Zhang J and Li S Y 2014 *Phys. Rev. Lett.* **113** 246402
[10] Wan X, Turner A M, Vishwanath A and Savrasov S Y 2011 *Phys. Rev. B* **83** 205101
[11] Lv B Q, Weng H M, Fu B B, Wang X P, Miao H, Ma J, Richard P, Huang X C, Zhao L X, Chen G F, Fang Z, Dai X, Qian T and Ding H 2015 *Phys. Rev. X* **5** 031013
[12] Xu S Y, Belopolski I, Alidoust N, *et al.* 2015 *Science* **349** 613
[13] Lv B Q, Xu N, Weng H M, Ma J Z, Richard P, Huang X C, Zhao L X, Chen G F, Matt C E, Bisti F, Strocov V N, Mesot J, Fang Z, Dai X, Qian T, Shi M and Ding H 2015 *Nat. Phys.* **11** 724
[14] Huang X, Zhao L, Long Y, Wang P, Chen D, Yang Z, Liang H, Xue M, Weng H, Fang Z, Dai X and Chen G 2015 *Phys. Rev. X* **5** 031023
[15] Yang L, Liu Z K, Sun Y, Peng H, Yang H F, Zhang T, Zhou B, Zhang Y, Guo Y F, Rahn M, Prabhakaran D, Hussain Z, Mo S K, Felser C, Yan B and Chen Y L 2015 *Nat. Phys.* **11** 728
[16] Huang S M, Xu S Y, Belopolski I, Lee C C, Chang G, Wang B K, Alidoust N, Bian G, Neupane M, Zhang C, Jia S, Bansil A, Lin H and Hasan M Z 2015 *Nat. Commun.* **6** 7373
[17] Xu S Y, Belopolski I, Sanchez Daniel S, *et al.* 2015 *Sci. Adv.* **1** e1501092
[18] Weng H, Fang C, Fang Z, Bernevig B A and Dai X 2015 *Phys. Rev. X* **5** 011029
[19] Liu Z K, Yang L X, Sun Y, Zhang T, Peng H, Yang H F, Chen C, Zhang Y, Guo Y F, Prabhakaran D, Schmidt M, Hussain Z, Mo S K, Felser C, Yan B and Chen Y L 2016 *Nat. Mater.* **15** 27
[20] Shekhar C, Nayak A K, Sun Y, Schmidt M, Nicklas M, Leermakers I, Zeitler U, Skourski Y, Wosnitza J, Liu Z, Chen Y, Schnelle W, Borrmann H, Grin Y, Felser C and Yan B 2015 *Nat. Phys.* **11** 645
[21] Arnold F, Shekhar C, Wu S C, Sun Y, Ricardo D d R, Kumar N, Naumann M, Ajeesh M O, Schmidt M, Grushin A G, Bardarson J H, Baenitz M, Sokolov D, Borrmann H, Nicklas M, Felser C, Hassinger E and Yan B 2016 *Nat. Commun.* **7** 11615
[22] Yang X, Liu Y, Wang Z, Zheng Y and Xu Z 2015 arXiv: 1506.03190v1 [cond-mat.mtrl-sci]
[23] Sun Y, Wu S C and Yan B 2015 *Phys. Rev. B* **92** 115428
[24] Zhang J, Liu F L, Dong J K, Xu Y, Li N N, Yang W G and Li S Y 2015 *Chin. Phys. Lett.* **32** 097102
[25] Zhang Y, Tan Y W, Stormer H L and Kim P 2005 *Nature* **438** 201

[26] Miller D L, Kubista K D, Rutter G M, Ruan M, de Heer W A, First P N and Stroscio J A 2009 *Science* **324** 924
[27] Wang K, Graf D, Wang L, Lei H, Tozer S W, Petrovic C 2012 *Phys. Rev. B* **85** 041101
[28] He J B, Wang D M and Chen G F 2012 *Appl. Phys. Lett.* **100** 112405
[29] Feng Ya, Wang Z, Chen C, *et al.* 2014 2014 *Sci. Rep.* **4** 5385
[30] Lee G, Farhan M A, Kim J S and Shim J H 2013 *Phys. Rev. B* **87** 245104
[31] Park J, Lee G, Wolff-Fabris F, et al. 2011 *Phys. Rev. Lett.* **107** 126402
[32] Wang K, Graf D, Lei H, Tozer S W and Petrovic C 2011 *Phys. Rev. B* **84** 220401
[33] Wang J K, Zhao L L, Yin Q, Kotliar G, Kim M S, Aronson M C and Morosan E 2011 *Phys. Rev. B* **84** 064428
[34] Guo Y F, Princep A J, Zhang X, et al. 2014 *Phys. Rev. B* **90** 075120
[35] Masuda H, Sakai H, Tokunaga M, et al. 2016 *Sci. Adv.* **2** e1501117
[36] May A F, McGuire M A, Sales B C 2014 *Phys. Rev. B* **90** 075109
[37] Wang K, Graf D and Petrovic C 2013 *Phys. Rev. B* **87** 235101
[38] Borisenko S, Evtushinsky D, Gibson Q, Yaresko A, Kim T, Ali M, Buechner B, Hoesch M and Cava R J 2015 arXiv: 1507.04847v2 [cond-mat.mes-hall]
[39] Liu J Y, Hu J, Zhang Q, Graf D, Cao H B, Radmanesh S M A, Adams D J, Zhu Y L, Chen G F, Liu X, Wei J, Tennant D A, DiTusa J F, Chiorescu I, Spinu L and Mao Z Q 2015 arXiv: 1507.07978v2 [cond-mat.mtrl-sci]
[40] Cordier G and Schäfer H 1977 *Z. Naturforsch.* **32** 383
[41] Zhang G M, Su Y H, Lu Z Y, Weng Z Y, Lee D H and Xiang T 2009 *Europhys. Lett.* **86** 37006
[42] Abrikosov A A and Beknazarov A 1988 *Fundamentals of the Theory of Metals* (Amsterdam: North Holland)
[43] Abrikosov A A 1998 *Phys. Rev. B* **58** 2788
[44] Abrikosov A A 2000 *Europhys. Lett.* **49** 789
[45] Hu J and Rosenbaum T 2008 *Nat. Mater.* **7** 697
[46] Lee M, Rosenbaum T F, Saboungi M L and Schnyders H S 2002 *Phys. Rev. Lett.* **88** 066602
[47] Huynh, Khuong K. and Tanabe, Yoichi and Tanigaki, Katsumi 2011 *Phys. Rev. Lett.* **106** 217004
[48] Li L, Wang K, Graf D, Wang L, Wang A and Petrovic C 2016 *Phys. Rev. B* **93** 115141